Investigating the effects of space weathering in Ryugu samples using coordinated microanalyses.

L. E. Melendez[1], M. S. Thompson[1], L. P. Keller[2], S. A. Eckley[3], and C. J. Snead[2]
[1]*Department of Earth, Atmospheric, and Planetary Sciences, Purdue University, West Lafayette, IN (melendl@purdue.edu)*
[2]*ARES, NASA Johnson Space Center, Houston, TX*
[3]*Jacobs, NASA Johnson Space Center, Houston, TX.*

Introduction: Airless planetary surfaces are characterized by a distinct lack of an atmosphere or magnetic field, leading to direct exposure to the effects of hypervelocity micrometeoroid impacts and solar wind ion irradiation [1]. These processes, cumulatively known as space weathering, gradually alter the microstructural and chemical properties of the grains on airless surfaces. Signatures of space weathering include vesiculated textures, amorphous grain rims (upper ~100 nm), solar flare tracks, and Fe-bearing nanoparticles (npFe) [2,3]. The accumulation of these microstructural space weathering characteristics, particularly the presence of npFe, alters the spectral properties of airless regoliths resulting in changes in spectral slope and reflectance of the surfaces, and the attenuation of characteristic absorption bands in the visible to near-infrared (Vis-NIR) wavelengths. These spectral changes complicate our ability to accurately interpret the mineralogy of airless bodies via remote sensing spectroscopy [1,4]. Studies of space weathering have primarily focused on anhydrous silicate minerals, reflecting the main components of the available returned samples from the Moon and S-type asteroid Itokawa [3,5,6]. However, our understanding of space weathering of primitive, organic-rich carbonaceous materials is still a work in progress. The Japan Aerospace Exploration Agency (JAXA)'s Hayabusa2 mission offered the first opportunity to directly investigate carbonaceous asteroids by returning samples from C-type asteroid (162173) Ryugu. Initial studies of Ryugu samples show mineralogical similarities to CI chondrites along with surface modifications consistent with space weathering. These surface modifications are primarily in the form of μm-thick silicate melts, amorphized phyllosilicates, glassy spherules, and burst vesicles [3,7]. Here, we report results from coordinated microanalytical techniques to further our understanding of the mineralogy and space weathering of carbonaceous materials.

Samples and Methods: We have been allocated two Ryugu particles returned by Hayabusa2; one particle collected at each of the two touchdown sites (A0152 and C0178). To understand the internal microstructure, mineralogy, and surface morphology of the two particles, we used X-ray computed tomography (XCT) to scan the samples using the Nikon XTH 320 micro-XCT at NASA Johnson Space Center (JSC) (Fig. 1). We also completed a higher-resolution sub-volume scan on the Zeiss Xradia 620 Versa at the University of Texas at Austin High Resolution X-ray CT Facility (UTCT) (Fig. 1). We segmented the dataset to identify different phases (e.g., sulfide minerals) and their spatial distribution using Dragonfly software. Due to the friable nature of the sample, small fragments were shed from the main mass during sample transport. We transferred <500 μm fragments of each particle to SEM mounts covered with carbon tape and coated the fragments with evaporated carbon. The stubs were characterized using the Quanta 3D FEG focused ion beam scanning electron microscope (FIB-SEM) at NASA JSC using both backscatter (BSE) and secondary electron (SE) imaging detectors along with a 70 mm^2 SDD energy dispersive X-ray spectroscopy (EDS) detector (Fig. 2).

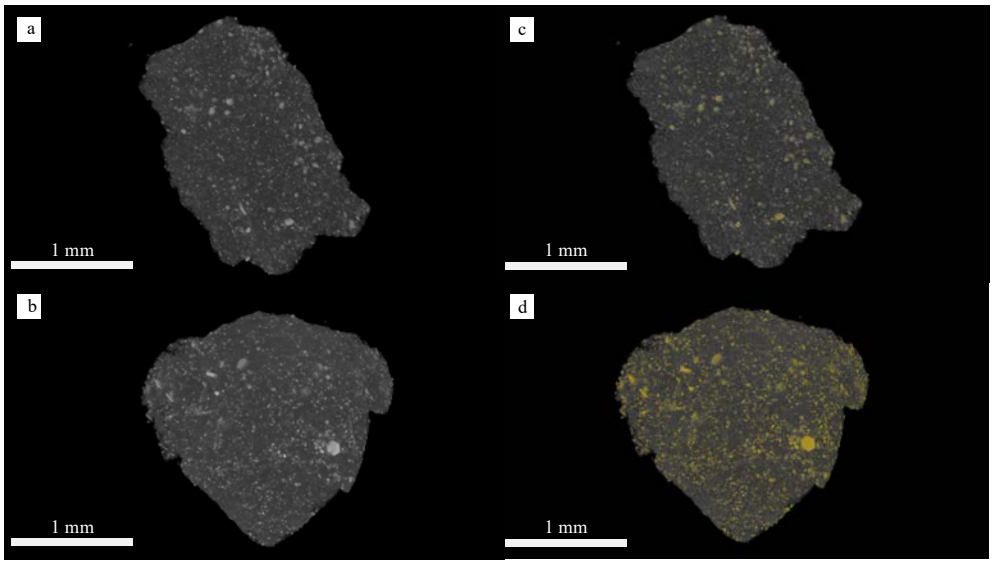

Figure 1. XCT scan of grain A0152 (a) and C0178 (b) with a resolution of 2.15 μm per voxel. Volume renderings with bright (higher relative Z number) phases (i.e., pyrrhotite and magnetite) in yellow for A0152 (c) and C0178 (d).

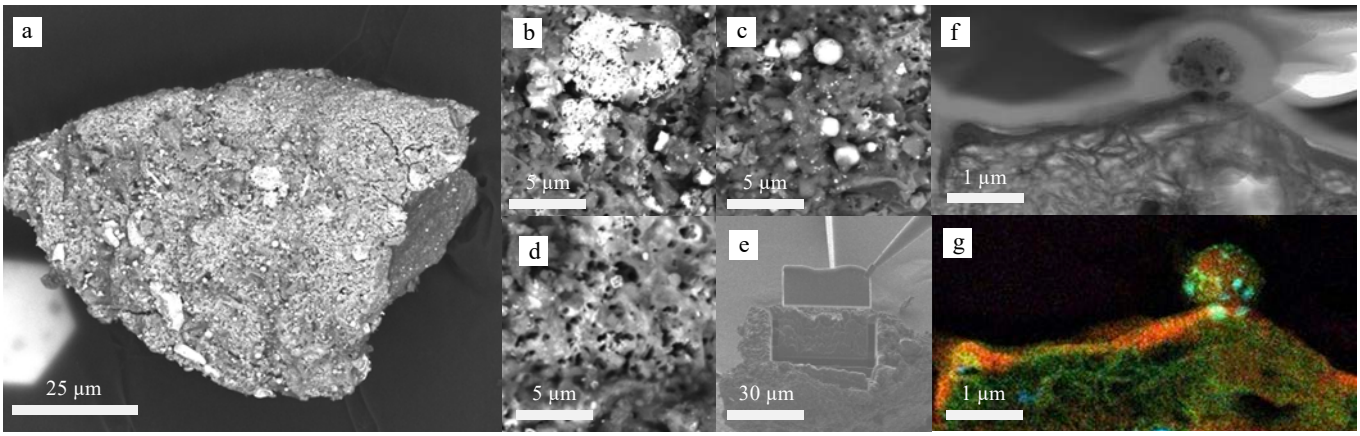

Figure 2. (a) Backscattered electron image (BEI) of one of the subparticles from A0152 with $Fe_{1-x}S$ (e.g., pyrrhotite (b)) and characteristic signatures of space weathering, including (c) melt droplets and (d) vesicular textures. This melt deposit was targeted for further analysis in the TEM, with electron transparent thin sections prepared using FIB-SEM (e). The BF STEM image from the resulting FIB section (f) shows a region with a sub-µm impact spherule on the surface on top of a darker melt layer. The composite RGB image (g) shows Mg (red), Fe (green), and S (blue), revealing a Mg-rich melt layer and a spherule with nanophase Fe and FeS inclusions.

Particles from chamber A that displayed vesicles or melt textures on their surface (indicators of micrometeoroid bombardment) were targeted for the preparation of three focused ion beam (FIB) sections for further analysis in the scanning transmission electron microscope (STEM). Particles from chamber C reflected the expected mineralogy of Ryugu but evidence of space weathering has not been identified on these grains. Two FIB sections were extracted from the phyllosilicate matrix and magnetite grains for comparison to the space-weathered regions of A0152. Bright field (BF) and dark field (DF) STEM images and chemical maps of the FIB sections were acquired using the JEOL 2500SE STEM equipped with a 60 mm^2 ultra-thin window silicon drift energy-dispersive EDS detector at JSC.

Discussion and Conclusions: XCT results indicate that the grain is a micro-breccia, and that hexagonal sulfide grains (likely pyrrhotite) are ~10 to ~200 µm wide are distributed throughout the fine-grained phyllosilicate and carbonate-rich matrix. Magnetite (Fe_3O_4) particles were also observed in both samples, exhibiting both framboidal and plaquette morphologies. 3D shape (SPO) and crystallographic (CPO) preferred orientations of sulfides (Fig. 1b) are being analyzed using Blob3D and 3DGrainMapper software, respectively. Currently, surface mesh renderings of A0152 and C0178 are being explored for evidence of impact cratering events, following [8]. SEM analysis of fragments from A0152 revealed vesiculated melt layers and frothy melt textures with melt spherules with embedded nanoparticles, resembling the deposits observed in simulated micrometeoroid bombardment [9]. STEM imaging confirmed the presence of Mg-rich phyllosilicates (serpentine and saponite), magnetite with variable morphologies, sulfides, and dolomite, consistent with previous studies of Ryugu samples indicating a low temperature aqueous alteration history [10, 11]. EDS analyses of these FIB sections of these regions revealed impact spherules and melt layers (up to 200 nm thick) containing abundant nanophase Fe-S and Fe-Ni-sulfides. Many of the nanoparticles are polyphasic, as opposed to the monomineralic nanoparticles observed in experimental samples. The melt layers have varying compositions depending on the underlying grain matrix: phyllosilicate grains have Ni-rich and Fe-poor melt layers while carbonate grains have Fe-, Mg- and O-rich melt layers. None of the particles analyzed thus far from C0178 exhibit textures characteristic of space weathering, which may be due to the comparatively 'fresh' nature of the subsurface sampling site, but we plan on proposing for additional grains for further analysis. We will continue to analyze these samples to better understand the effects of space weathering on carbonaceous regolith in preparation for the analysis of returned samples from asteroid Bennu by OSIRIS-REx this year.

References

[1] Pieters C. M. and Noble S. K. (2016) *Journal of Geophysical Research* 121(10): 1865–1884. [2] Keller L. P. and McKay D. S. (1997) *Geochimica et Cosmochimica Acta* 61:2331–2341. [3] Noguchi T. et al. (2014) *Meteoritics & Planetary Science* 49:188–214. [4] Chapman C. R. (2004) *Annual Review of Earth and Planetary Sciences* 32:539–567. [5] Taylor L. A. et al. (2001) *Journal of Geophysical Research: Planets* 106:27985–27999. [6] Nakamura, T. et al. (2011) *Science* 333: 1113–1116. [7] Matsumoto, T. et al. (2021) *Hayabusa Symposium 2021*. NIPR.[8] Hamann, C. et al. (2023) *86th Annual Meeting of the Meteoritical Society Conference* Abstract 2692. [9] Thompson M.S. et al. (2019) *Icarus* 319: 499–511. [10] Matsumoto T. et al. (2021) *Nature Communications* 11:1–8. [11] Nakamura T. et al. (2022) *Science* 379: 6634–6785. [12] Tomioka et al. (2023) *Nature Astronomy* 7: 669–677.